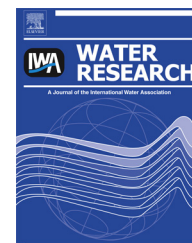


Available online at [www.sciencedirect.com](http://www.sciencedirect.com)

SciVerse ScienceDirect

journal homepage: [www.elsevier.com/locate/watres](http://www.elsevier.com/locate/watres)

# Lorazepam photofate under photolysis and TiO<sub>2</sub>-assisted photocatalysis: Identification and evolution profiles of by-products formed during phototreatment of a WWTP effluent

M.A. Sousa<sup>a,b</sup>, O. Lacina<sup>c</sup>, P. Hrádková<sup>c</sup>, J. Pulkrabová<sup>c</sup>, Vítor J.P. Vilar<sup>d</sup>, C. Gonçalves<sup>b</sup>, Rui A.R. Boaventura<sup>d</sup>, J. Hajšlová<sup>c</sup>, M.F. Alpendurada<sup>b,\*</sup>

<sup>a</sup> Department of Bromatology and Hydrology, Faculty of Pharmacy, University of Porto, Rua de Jorge Viterbo Ferreira 228, 4050-313 Porto, Portugal

<sup>b</sup> IAREN – Water Institute of the Northern Region, Rua Dr. Eduardo Torres 229, 4450-113 Matosinhos, Portugal

<sup>c</sup> Department of Food Analysis and Nutrition, Institute of Chemical Technology, Technická 3, 166 28 Praha 6, Czech Republic

<sup>d</sup> Laboratory of Separation and Reaction Engineering – Associate Laboratory LSRE/LCM, Faculty of Engineering, University of Porto, Rua Dr. Roberto Frias, 4200-465 Porto, Portugal

## ARTICLE INFO

### Article history:

Received 4 March 2013

Received in revised form

13 June 2013

Accepted 17 June 2013

Available online 26 June 2013

### Keywords:

Lorazepam

TiO<sub>2</sub>-photocatalysis

CPCs solar pilot plant

By-products

Ultra-high performance

liquid chromatography–high

resolution mass spectrometry

## ABSTRACT

This manuscript reports on the study of Lorazepam (LZP) phototransformation pathways under artificial UV and natural solar irradiation, through photolytic and TiO<sub>2</sub>-assisted photocatalytic processes. Three experimental set-ups were employed: two lab-scale photoreactors, each provided with an UV lamp (one medium pressure mercury lamp and one blacklight blue lamp), and a pilot-scale Solar Plant with Compound Parabolic Collectors (CPCs). Samples collected along the different phototreatment experiments were analyzed by ultra-high performance liquid chromatography–quadrupole-time-of-flight–mass spectrometry (UHPLC/QqToF-MS). The key assumption of the analytical approach was that related compounds (LZP and its by-products (LBPs)) provide identical “diagnostic fragment ions”. Identification was also based on the chlorine atoms specific isotopic pattern, as well as accurate masses. Six major LBPs were identified and elucidated, with nominal [M + H]<sup>+</sup> masses of 337, 303, 319, 275, 291 and 293 Da. The proposed LZP photodegradation mechanism included the initial opening of the diazepinone seven-membered ring, followed by a rearrangement into a highly stabilized six-membered aromatic ring and subsequent cleavage and/or hydroxylation reactions. The evolution profiles of LBPs were described for each of the three experimental prototypes and the CPCs Solar Pilot Plant proved to be the most efficient one. Finally, LZP photocatalytic degradation was further assessed on a municipal effluent, where the photoproducts generated showed to be more persistent than LZP itself.

© 2013 Elsevier Ltd. All rights reserved.

\* Corresponding author. Tel.: +351 229 36 42 10; fax: +351 22 936 42 19.

E-mail addresses: [mfalpendurada@iaren.pt](mailto:mfalpendurada@iaren.pt), [geral@iaren.pt](mailto:geral@iaren.pt) (M.F. Alpendurada).  
0043-1354/\$ – see front matter © 2013 Elsevier Ltd. All rights reserved.  
<http://dx.doi.org/10.1016/j.watres.2013.06.029>

## 1. Introduction

Pharmaceuticals have become prominent emerging contaminants due to their demonstrated presence and persistence in environmental waters, as well as for the potential toxicological effects they may induce on non-target organisms. Some major concerns have been raised regarding their possible estrogenic effects, not to mention the development of different bacterial resistances (creation of “Super Bugs”). It is currently estimated that approximately 3000 different compounds are used as pharmaceutically active substances, including analgesics, antibiotics, anxiolytics, antidepressants,  $\beta$ -blockers, lipid regulators, antidiabetics, neuroleptics, contraceptives and impotence drugs. Nevertheless, still only a rather small subset of these compounds has been investigated in environmental studies (Richardson and Ternes, 2011).

Due to the growing competitiveness installed in modern society, the consumption of anxiolytic drugs has recently shown a remarkable increase. According to the International Narcotics Control Board (International Narcotics Control Board, 2010), in 2008 a total of 30 billion S-DDD (defined daily doses for statistical purposes) of benzodiazepines (BDZ) were manufactured, the highest amount registered up until today. Moreover, Portugal was considered one of the countries with the highest anxiolytics consumption rate (International Narcotics Control Board, 2010). Amongst the most marketed anxiolytic drugs in Portugal, Lorazepam (LZP) highlights with a quite high sales value over the past 5 years, according to unpublished data provided by the Portuguese National Authority of Medicines and Health Products, IP (INFARMED).

Pharmaceutical compounds in general reach the aquatic media, where they have been found in concentrations ranging from  $<0.1$  to ca.  $20 \mu\text{g L}^{-1}$ , among treated wastewaters, surface and groundwater and even drinking water (Castiglioni et al., 2005; Gros et al., 2006; Kasprzyk-Hordern et al., 2009; Webb et al., 2003; Zuehlke et al., 2007). LZP, in particular, has already been quantified in levels ranging from approximately  $0.040 \mu\text{g L}^{-1}$  in river waters to ca.  $0.200 \mu\text{g L}^{-1}$  in effluent wastewaters (Silva et al., 2011; Coetsier et al., 2009; Valcárcel et al., 2012). The environmental aquatic pollution by such persistent organic pollutants is commonly attributed either to point-source contaminations or following the incomplete removal in wastewater treatment plants (WWTPs). In fact, WWTPs are not prepared for the complete degradation of such micropollutants, as mentioned in several studies (Ternes, 1998; Santos et al., 2009; Gros et al., 2010).

The limitations of conventional wastewater treatments for the remediation of emerging pollutants require the development and application of advanced tertiary/quaternary treatment processes. In this field, special attention has been given to Advanced Oxidation Processes (AOPs), in which hydroxyl radicals ( $\text{HO}^\bullet$ ) are the responsible agents for the oxidation and mineralization of almost any organic molecule, due to their strong unselective oxidative power, yielding  $\text{CO}_2$  and inorganic ions as final products (Vilar et al., 2011). Common techniques already reported in the literature include the use of UV alone, UV/ $\text{TiO}_2$ , UV/ $\text{H}_2\text{O}_2$ , UV/ $\text{Fe}^{3+}$ , UV/ $\text{H}_2\text{O}_2/\text{Fe}^{3+}$ , UV/ $\text{S}_2\text{O}_8^{2-}$ , UV/chlorine and UV in combination with other photocatalysts (Lau et al., 2007; Cooper et al., 2008). Among them,

the heterogeneous photocatalysis with UV/ $\text{TiO}_2$  showed to be a promising technique for wastewater detoxification (Malato et al., 2009).  $\text{TiO}_2$  has generally been considered the most active catalyst, whenever tested against other semiconductor materials, under comparable conditions (Galvez and Malato, 2003). However, despite the fact that AOPs are being widely used in wastewater treatment for the removal of both organic and inorganic contaminants, as well as to increase effluents' biodegradability, a partial oxidation may result in the formation of intermediates more toxic than parent compounds (Rizzo, 2011). For this reason, it becomes indispensable to identify the resulting photoproducts, in order to allow the study of their individual/mixture toxicity.

The work herein described aims at the elucidation of LZP photodegradation mechanism. LZP phototreatment was performed via different processes, including solar UV light vs. artificial UV radiation sources, as well as photolytic vs. photocatalytic pathways. The identification of the main photoproducts was carried out by ultra-high performance liquid chromatography–quadrupole-time-of-flight–mass spectrometry (UHPLC/QqToF-MS) and their formation was followed up concomitantly with the degradation of the parent compound. To the best of the authors' knowledge, this work has never been undertaken before. Furthermore, LZP photodegradation products were also analyzed over the phototreatment of a real municipal WWTP effluent.

## 2. Experimental

### 2.1. Chemicals and materials

LZP used in the experiments was in the form of standard solution  $1 \text{ mg mL}^{-1}$  supplied by LGC Standards (Barcelona, Spain) and Lorenin<sup>®</sup> pills (1 mg) were from Wyeth. The pills were also composed of lactose monohydrate, microcrystalline cellulose, polacrillin potassium and magnesium stearate (ca. 100 mg). Consequently, a more realistic scenario was simulated using the pills, and any possible interference due to the presence of the 4 excipients has not been disregarded.  $\text{TiO}_2$  catalyst (P25 Degussa, 80% anatase and 20% rutile) was purchased from Degussa Portuguesa. Demineralized and ultra-pure water, used in the phototreatment experiments, were obtained with a reverse osmosis system (Panice<sup>®</sup>) and a Millipore<sup>®</sup> system (Direct-Q model), respectively. Methanol (LiChrosolv<sup>®</sup>) for UHPLC/QqToF-MS analyses was LC gradient grade purchased from Merck. Formic acid ( $\sim 98\%$  purity) and ammonium acetate ( $>99.9\%$  purity) were both purchased from Sigma–Aldrich (Germany). Nylon syringe filters ( $0.2 \mu\text{m}$ ) were provided by VWR International. Temperature and pH data were collected using a pH meter HANNA HI8424.

### 2.2. Photodegradation systems

In this work, three distinct experimental set-ups were used to induce LZP photodegradation. The first lab-scale experimental apparatus consisted of a glass immersion photochemical reactor with a water column of 8 cm diameter and 16 cm height. The reactor was loaded with 850 mL of solution, with

constant stirring for the total reaction period. It was equipped with a medium pressure mercury lamp Heraeus TQ150W, with a dominant emission line at 366 nm, placed axially and held in a quartz immersion tube with a surface contact area of  $\sim 233 \text{ cm}^2$  – LsTQUV (Lab-scale TQ150W-UV prototype) (Fig. S1a). This system was refrigerated by a continuous tap water flow, which allowed temperature to be properly controlled below  $30^\circ\text{C}$ . The second employed lab-scale prototype was composed by a 5 L beaker, loaded with 4.5 L of solution constantly stirred, and an immersed pyrex glass cylinder placed axially, holding an LYNX S 11W blacklight blue lamp with maximal emission at 365 nm. The surface contact area between the pyrex cylinder and the solution was approximately  $456 \text{ cm}^2$ . The water column was 23.5 cm high with 11 cm diameter – LsBLBUV (Lab-scale Blacklight Blue-UV system) (Fig. S1b).

Furthermore, photocatalytic experiments were also performed, during sunny days, in a Solar Pilot Plant with Compound Parabolic Collectors, installed in the roof of the Chemical Engineering Department of the Faculty of Engineering, University of Porto (FEUP), Portugal. This solar collector ( $0.91 \text{ m}^2$ ) was composed of four borosilicate tubes (Schott-Duran type 3.3, Germany, cut-off at 280 nm, external diameter 50 mm, length 1500 mm and thickness 1.8 mm) connected in series by polypropylene junctions with their mirrors in anodized aluminum, supported by an aluminum structure and tilted  $41^\circ$  (local latitude) – SPP-CPCs (Solar Pilot Plant with Compound Parabolic Collectors) (Fig. S1c).

More detailed information regarding the characteristics of the used UV lamps and the design/functioning of the described phototreatment experimental set-ups can be found in previous publications (Pereira et al., 2011; Pinho et al., 2012).

### 2.3. Photodegradation experiments and procedure

Irradiation experiments with LZP were performed using the three described systems: LsTQUV, LsBLBUV and SPP-CPCs (refer to Section 2.2.). Prior to use, Lorenin® pills were ground using a porcelain pestle and mortar.

For the LsTQUV experiment, 5 Lorenin® pills were dissolved in 100 mL Milli-Q water and LZP was extracted with 100 mL ethyl acetate (solubility of  $30 \text{ mg mL}^{-1}$  in ethyl acetate and  $0.08 \text{ mg mL}^{-1}$  in water) (Budavari et al., 1989), using a separatory funnel. Ethyl acetate was then completely evaporated and LZP redissolved in Milli-Q water, up to a final volume of 850 mL ( $[\text{LZP}]_{\text{final}} \sim 6 \text{ mg L}^{-1}$ ). After constant stirring of the solution, in the dark (lamp-off) for approximately 15 min, using the described LsTQUV system, a first sample was collected (time 0), after which the photolytic process began by turning the UV light on, while different samples were taken, every minute during 20 min. Moreover, a similar experiment was performed with the total Lorenin® pills (LZP plus excipients). In this case, a dark control experiment under analogous experimental conditions was also conducted. In the case of the LsBLBUV experiment, 22 Lorenin® pills were dissolved in 4.5 L of Milli-Q water ( $[\text{LZP}]_{\text{final}} \sim 5 \text{ mg L}^{-1}$ ) and further submitted to a photocatalytic treatment with  $200 \text{ mg L}^{-1}$  of  $\text{TiO}_2$  (in suspension). Likewise, the suspension was continuously stirred during the whole experiment and several samples were collected, at different time intervals, after turning the UV

light on. According to previous results (Sousa et al., 2013), LZP undergoes neither significant hydrolysis nor adsorption onto the catalyst surface, thus in the present work no control sample was collected after the catalyst addition and prior to the beginning of irradiation. Lastly, in the case of the SPP-CPCs system, 30 Lorenin® pills were dissolved in 15 L of distilled water ( $[\text{LZP}]_{\text{final}} \sim 2 \text{ mg L}^{-1}$ ) and photocatalytic experiments were performed with  $200 \text{ mg L}^{-1}$  of  $\text{TiO}_2$  (experimentally determined optimal  $\text{TiO}_2$  concentration) (Sousa et al., 2013). The suspension was constantly mixed by turbulent recirculation ( $\sim 0.3 \text{ min}$  residence time,  $\sim 40\%$  illuminated volume). Finally, experiments began by uncovering the CPCs and different aliquots were collected at pre-defined times. Afterward, a similar experiment was performed over a real municipal WWTP effluent sample, further spiked with Lorenin® pills in order to attain a final LZP concentration of ca.  $2 \text{ mg L}^{-1}$ . No pH adjustments were performed in any of the photodegradation processes. Temperature and pH were continuously monitored along all experiments.

Prior to LC–MS/MS analysis, all sample aliquots containing  $\text{TiO}_2$  were pre-filtered through  $0.2 \mu\text{m}$  membrane filters. Afterward, LZP and its photoproducts were analyzed using the UHPLC/QqToF-MS system.

### 2.4. UHPLC/QqToF-MS analysis

Ultra-high performance liquid chromatography analyses, carried out to resolve LZP and its phototransformation products, were performed by Dionex UltiMate 3000 RS UHPLC system (Thermo Fisher Scientific, Waltham, USA), equipped with a  $100 \text{ mm} \times 2.1 \text{ mm i.d.}$ ,  $1.8 \mu\text{m}$  particle size Acquity UPLC® HSS T3 column (Waters, Milford, MA, USA), maintained at  $40^\circ\text{C}$ . The mobile phases consisted of (A) 0.010 M formic acid in Milli-Q water for ESI(+) mode and 0.005 M ammonium acetate in Milli-Q water for ESI(–) analyses, and (B) methanol, with the following multi-step elution gradient: 0 min (98% A;  $0.30 \text{ mL min}^{-1}$ ), 8.0 min (0% A;  $0.45 \text{ mL min}^{-1}$ ), 10.0 min (0% A;  $0.45 \text{ mL min}^{-1}$ ), 10.1 min (98% A;  $0.40 \text{ mL min}^{-1}$ ) and a short column reconditioning period up to 12.0 min (98% A;  $0.40 \text{ mL min}^{-1}$ ). Nevertheless, this gradient was later adjusted to an initial methanol concentration of 20%, in order to better separate the many co-eluted peaks between ca. 5–8 min. The sample injection volume was  $10 \mu\text{L}$ , in all experiments, and the autosampler temperature was fixed at  $5^\circ\text{C}$ .

For the identification of LZP photoproducts, high-resolution MS analyses were performed using an ABSCIEX TripleTOF® 5600 (Toronto, ON, Canada), provided with a Duo Spray™ ion source, operated in positive mode. The ion source was set at the following conditions: ion-spray voltage floating (ISVF) 4 kV, temperature (TEM)  $600^\circ\text{C}$ , ion source gases (GS1 and GS2) 60 psi, curtain gas (CUR) 35 psi and a declustering potential (DP) of 60 V.

### 2.5. LZP by-products elucidation strategy

The initial screening method consisted of two TOF MS (+) scan simultaneous experiments, the second with induced fragmentation (collision energy (CE) of 35 V). Acquired  $m/z$  values ranged between 50 and 650 Da, with an accumulation time of 0.25 s and a total acquisition time of ca. 12 min. The chosen

samples for these primary analyses were selected from an intermediate phototreatment time, so that they were likely to contain a significant amount of some LZP degradation products. Afterward, with the attained information regarding LZP characteristic/diagnostic fragment ions, associated to exact mass results, it was possible to determine a great variety of molecular ions. Subsequently, information dependent acquisition (IDA) method was employed to collect full scan MS and MS/MS information simultaneously and allow their following quantitative analysis. The method consisted of a survey TOF MS (+) experiment from  $m/z$  100 to  $m/z$  650 and product ion (PI) spectra for the eight most intense ions of the survey spectra throughout the chromatographic run. Dynamic background subtraction was activated to automatically acquire PI spectra of co-eluting compounds. PI spectra were collected only ions from  $m/z$  150 to  $m/z$  400, moreover the isotopes within 1 Da and the former precursor ion were excluded for 5 s (mass tolerance of 30 mDa) and totally excluded after three occurrences. This setting allowed acquisition of thousands of unique  $m/z/t_R$  combinations. The collision energy of 35 V with a collision energy spread of  $\pm 15$  V was used for the PI spectra. The collision energy spread resulted in more characteristic MS/MS spectra since both low and high energy fragment ions were present in a single spectrum. Since the total cycle (survey scan and 8 PI spectra) took only 0.55 s, at least 12 points per peak were always achieved for accurate quantitation.

An automatic  $m/z$  calibration was performed every ten samples with the positive APCI calibration solution, using the calibration delivery system (CDS), and each set of samples was preceded by two blank controls: Milli-Q water and methanol. In the end, the same MS approach was conducted in ESI(–) mode, though the resulting chromatograms presented no relevant additional information. The MS detector was used, in both ESI(+) and ESI(–) modes, the resolving power was  $>31,000$  ( $m/z$  321.0192) full width at half maximum (FWHM). Since the PI spectra were measured in high sensitivity mode, half resolution was obtained.

Instrument control and data acquisition were carried out with the AnalystV1.5.1 TF software (ABSciex) and the qualitative analysis was performed using PeakView, also equipped with the XIC Manager and Formula Finder tools. All identified LZP degradation products were further quantitatively processed using MultiQuantV2.1 software.

### 3. Results and discussion

#### 3.1. Preliminary results and analytical approach

According to previous results described by Sousa et al. (2013), using the LsTQUV apparatus, LZP highest degradation yield is obtained through photolysis, while with the SPP-CPCs system the best degradation performance is achieved through a photocatalytic process, using a  $\text{TiO}_2$  concentration of  $200 \text{ mg L}^{-1}$ . Besides, the degradation kinetic constant determined for the optimized method using the SPP-CPCs system ( $k = 1.49 \pm 0.03 \text{ L kJ}^{-1}$ ) was higher than the one calculated for the LsTQUV set-up ( $k = 0.131 \pm 0.006 \text{ L kJ}^{-1}$ ). In the case of the LsBLBUV apparatus, photocatalysis with a  $\text{TiO}_2$  concentration of  $200 \text{ mg L}^{-1}$  was elected as well, since LZP photolytic

degradation was still quite lengthy (data not shown). To further complement LZP phototreatment study, the purpose of the present work was to tentatively identify the different resulting photoproducts, postulate the actual LZP photodegradation pathway(s) and assess their occurrence in environmental matrices. In order to achieve so, the tested LZP concentrations were in the low ppm range ( $2\text{--}6 \text{ mg L}^{-1}$ ), despite significantly higher than the already reported aquatic environmental values (ca.  $40\text{--}200 \text{ ng L}^{-1}$ ).

As aforementioned, the employed non-target screening approach initially consisted of two TOF MS (+) scan simultaneous experiments, one with and one without in-source fragmentation. This interesting strategy, based upon the concept of “diagnostic fragment ions”, was first described by Ferrer and Thurman (2007). Applied to the present case-study, the key assumption is that LZP photodegradation products will still present a basic structure analogous to that of the parent compound and, consequently, a similar in-source fragmentation pattern. The resulting diagnostic fragment ions were then selected bearing in mind the presence of the chlorine atom specific isotopic pattern, as well as accurate masses. Subsequently, the corresponding molecular ions were identified in the respective non-fragmented sample chromatogram, using background subtraction at the corresponding retention times ( $t_R$ ) and taking into account peaks with identical shape (Lacina et al., 2010). Afterward, MS/MS spectra of every  $[M + H]^+$  ions were acquired by IDA product ion (+) MS analysis, as previously mentioned in Section 2.3. Finally, with the help of the Formula Finder tool, from the PeakView software, the structural enlightening of several LZP photoproducts was possible, taking into account LZP structural formula and respective tandem MS spectra, as well as some of the software proposed fragments with corresponding spectra fitting probabilities.

#### 3.2. Structural elucidation of LZP by-products and mechanism proposal

As previously mentioned, the samples selected for preliminary UHPLC/QqToF-MS analyses were chosen from an intermediate phototreatment time, in order to potentially contain a higher amount of most LZP photoproducts, and the selected system was the LsTQUV, since it allowed to start with higher LZP concentrations. Nevertheless, all compounds herein identified were later confirmed in most samples obtained in the remaining photocatalytic systems (LsBLBUV and SPP-CPCs), bearing in mind the same exact masses and  $t_R$ , in addition to comparable  $\text{MS}^2$  spectra.

Initially, several molecular ions were included in the group of potential LZP by-products (LBPs), though some of them were later identified as corresponding to either  $^{35}\text{Cl}/^{37}\text{Cl}$  isotopes or  $\text{Na}^+/\text{K}^+$  adducts of other  $[M + H]^+$  ions. Such examples were the cases of LZP itself ( $m/z$  321.0196 ( $^{35}\text{Cl}$ )/323.0167 ( $^{37}\text{Cl}$ )), presenting a sodium adduct at  $m/z$  343.0014/344.9984 and a potassium adduct at  $m/z$  358.9749/360.9723, as well as LBP291 ( $m/z$  291.0088/293.0058), with a sodium adduct at  $m/z$  312.9906/314.9877, or LBP319 ( $m/z$  319.0034/321.0007), with a sodium adduct at  $m/z$  340.9862/342.9828 (Fig. S2). For these preliminary identifications, besides taking into account the two chlorine atoms typical isotopic pattern, both isotopes exact masses ( $^{35}\text{Cl}$



isotope – 34.9689 and  $^{37}\text{Cl}$  isotope – 36.9659) were also considered. Thus, the selected ions were those corresponding to an isotope  $m/z$  difference slightly inferior to 2 Da. Furthermore, chromatographic data was also found to be an indispensable tool to enable the distinction between true LZP photoproducts and some potentially formed LZP in-source fragments. For instance, at first sight, the 303.0085  $m/z$  fragment could be considered a LBP, since it fitted all MS requisites imposed by the adopted analytical strategy. However, when comparing its chromatographic profile with LZP's, the obtained peaks were overlapping (i.e., similar shapes and  $t_R$ ), leading to the conclusion that this compound was merely the result of in-source fragmentation and not of the phototreatment process. Moreover, it was later confirmed that there was actually a LBP with a nominal mass of 303 Da, but its exact monoisotopic mass was still significantly higher (303.0560  $m/z$ ).

Finally, fourteen compounds (excluding structural isomers) were identified as presumable LBPs and none of the corresponding peaks was detected in either of the used control blanks. All TOF MS scan extracted ion chromatograms (XICs) are presented in Fig. S3. Herein, one can observe that these putative LBPs were mostly eluted in the narrow range between 4 and 7 min, even after some preliminary improvements in the chromatographic elution gradient (refer to Section 2.3.). Nonetheless, the QToF still afforded sufficient selectivity to record good quality product ion spectra for the majority of these compounds: LBP257, LBP266, LBP275, LBP282, LBP291, LBP293, LBP303, LBP319 and LBP337. The  $\text{MS}^2$  XIC and mass spectrum of LBP319 are displayed in Fig. 1, while those of LZP and remaining by-products are presented in Fig. S4. Other less abundant LBPs included LBP156, LBP223, LBP230, LBP239 and LBP273. Fig. S4 illustrates some examples of the use of diagnostic ions for the identification of non-target by-products obtained after phototreatment of the (targeted) parent compound LZP. One example was the case of the fragment ion 275.0171  $m/z$ , identified in the mass spectrum of LBP319. Other fragment ions such as 229.0547  $m/z$  and 163.0064  $m/z$  were identified as well in the mass spectra of LBP303 and LBP257/LBP275/LBP291, respectively. However, despite constituting a rather useful tool for finding structurally related compounds, namely degradation products, the applicability of the diagnostic fragment ions concept is slightly limited and many

exceptions exist (Lacina et al., 2010). Therefore, other important pieces of information such as chlorine isotopic pattern, exact masses, cleavage/oxidation and energetically favored reactions were considered when trying to establish some LBPs' structures.

In Fig. 1, the detected ion with a nominal mass of 319 Da was rationalized as being the product of the opening of the diazepinone seven-membered ring, followed by a rearrangement into a highly stabilized six-membered aromatic ring (LBP319) (Calisto et al., 2011). The resulting exposed carboxylic function is then likely to be cleaved, yielding an ion with 275 Da (LBP275) – neutral loss of 44 Da, corresponding to the carboxylic group. It should be highlighted that this photoproduct with monoisotopic mass of ca. 275.0175  $m/z$  corresponds also to a LZP in-source fragment, as one can observe on LZP PI spectrum and corroborated by the presence of the small peak at 5.76 min (LZP  $t_R$ ) in LBP275 chromatogram. This aspect stresses, once again, the importance of good resolution of the parent compound/photoproducts.

Concerning the remaining proposed LBPs, their structures were put forward based on the common reactions taking place in photocatalysis, namely oxidative processes mediated by  $\text{HO}^\bullet$  species. Consequently, from a mechanistic point of view, different hydroxylation reactions could be predicted. Regarding LBP337 and LBP303, they were considered side products of LZP phototreatment and interpreted as the result of the addition of a hydroxyl group to one of LZP's benzene rings and the substitution of one chlorine atom by the hydroxyl group, respectively. However, these hydroxylation reactions could take place at different carbons of LZP skeleton, leading to the formation of distinct isomeric hydroxyl derivatives and, thus, different chromatographic peaks (Lacina et al., 2010). As one can observe in Fig. S4, in the case of LBP337, it was possible to distinguish between two potential structural isomers, each one derived from hydroxylation of a different aromatic ring, leading to the identification of ions at  $m/z$  154.0078 and 179.0040 and corresponding putative structures. Still, the exact position of the  $-\text{OH}$  substituent in the benzene ring remains undetermined. On the other hand, in the case of LBP303, it was possible to pinpoint exactly which chlorine atom was being substituted by the hydroxyl group, thanks to the structures tentatively attributed to ions at  $m/z$  145.0388 and 153.0204

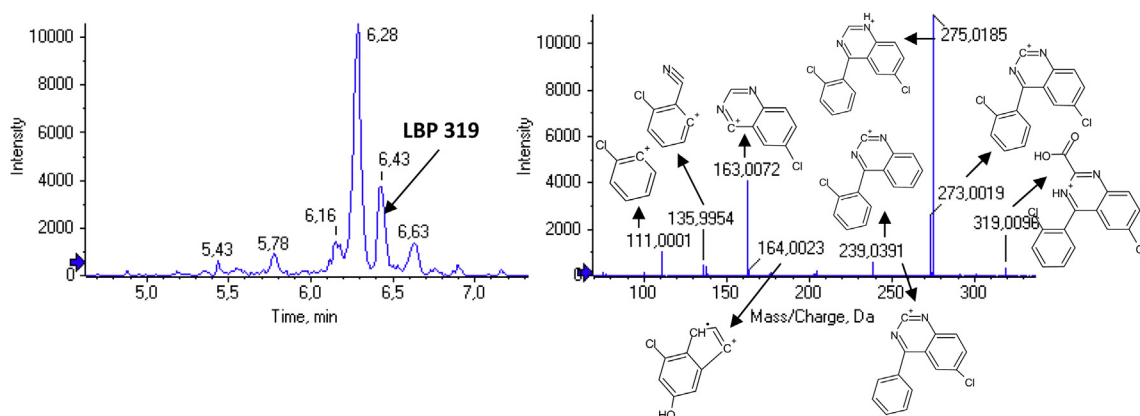


Fig. 1 – (+)ESI- $\text{MS}^2$  extracted ion chromatogram and mass spectrum of LBP319, obtained with sample  $Q_{UV} = 13.5 \text{ kJ L}^{-1}/\text{LsTQUV}$  prototype. Some putative structures are presented in the MS spectrum.

These ions were separately identified in the spectrum of each of the two most intense peaks, located at  $t_R$  3.65 and 5.92 min. With reference to the probable LBP291, also shown in Fig. S4, the three observed peaks were interpreted as three different structural isomers: the most intense peak at 6.92 min, most likely corresponding to the hydroxyl addition in the middle ring (LBP291(b)) according to the proposed structure for the 179.0009 Da ion, and two others at 6.05 and 6.46 min (LBP291(a)), matching the hydroxylation on each of the two additional aromatic rings. Nevertheless, the latter two structures were again indistinguishable. According to some results reported by Calisto et al. (2011), LBP266 was also identified in the present work, showing some common MS<sup>2</sup> fragments with another proposed LBP photoproduct – LBP282 (ions with the nominal mass of 154 and 126 Da) (Fig. S4). Thus, it was our belief that LBP282 may result from the hydroxylation of LBP266 in one of the aromatic rings. Finally, the structure proposed for the putative LBP257 differs significantly from that previously presented by Calisto et al. (2011), consisting of a fused tricyclic structure, while our suggestion is more coherent with earlier stage photoproducts. Besides, Calisto et al. (2011) have only simulated the environmental degradation of BDZ, including LBP, in the laboratory i.e., they disregarded accelerated photodegradation processes such as TiO<sub>2</sub>-driven photocatalysis, as well as any mechanistic elucidation.

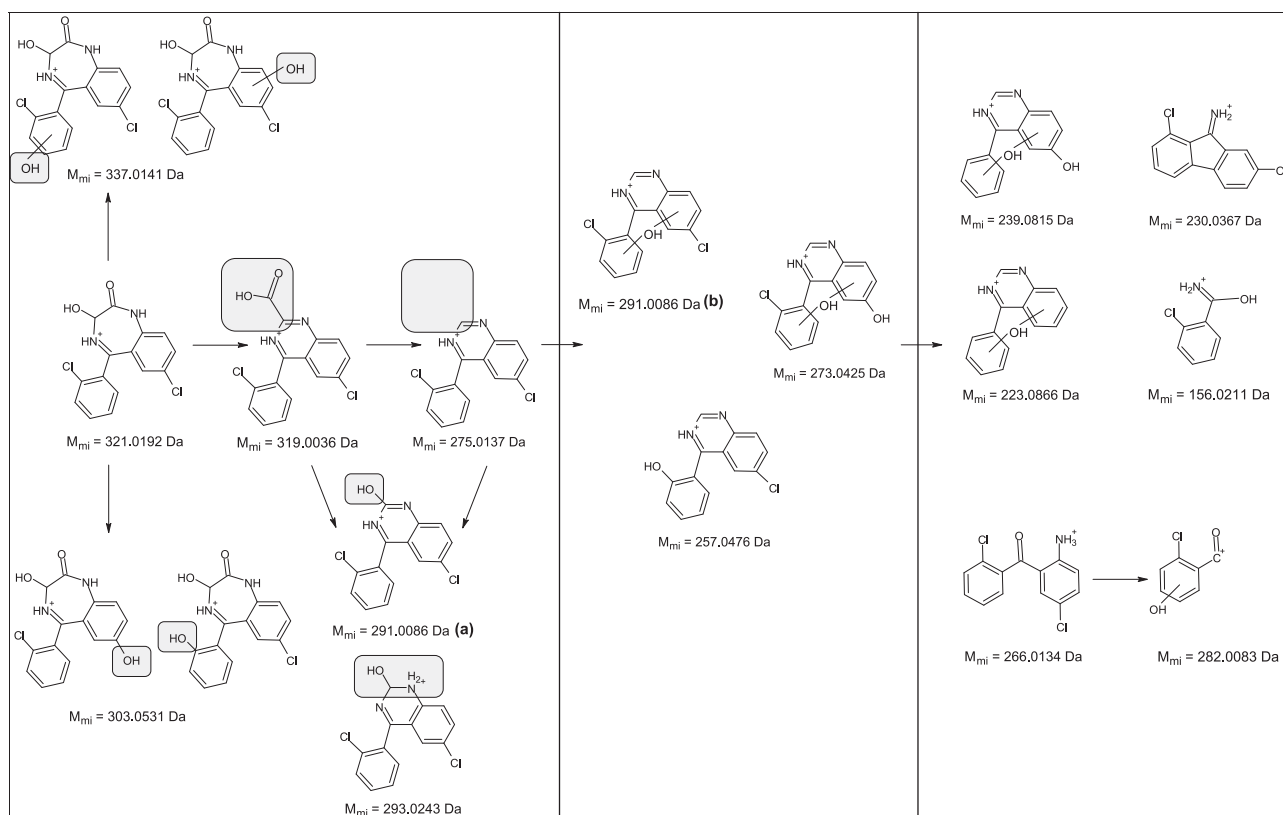
Considering the importance of having a holistic overview of LBP photofate in the environment, in the present work a photodegradation pathway is proposed (Scheme 1), based on

the results discussed so far. As it can be observed, the suggested scheme is divided in three main stages: a first one, leading to the formation of key LBP275, through the intermediate LBP319, including as well some LBP275 side products resulting from the hydroxylation of the central diamino-ring; a following stage, comprising LBP291, LBP257 and LBP273, corresponding to –OH addition, –Cl substitution and both, respectively; a third stage encompassing different photoproducts resulting from probable cleavage and/or hydroxylation reactions (LBP266, LBP282, LBP239, LBP230, LBP223 and LBP156).

In conclusion, the unambiguous identification and confirmation of some LBP photoproducts was enabled taking into account the parent compound structural formula and performing an accurate mass analysis of the protonated molecules, together with that of additional characteristic fragment ion(s), including characteristic isotopic signals and retention times.

### 3.3. Comparison between LsTQUV, LsBLBUV and SPP-CPCs experiments

The evolution profiles of the above enumerated LBP photoproducts and whether or not they were produced using the three employed experimental systems was then investigated. Since authentic standards are not commercially available for these LBPs, their concentrations in the several collected samples could not be accurately calculated. Thus, in Fig. 2 we illustrated their evolution in terms of peak area (i.e., ratio  $A_t$ /



**Scheme 1 – Proposed 3-steps pathway for the photo(cata)lytic conversion of LBP into the respective photoproducts [LBP anxiolytic drug: (RS)-9-chloro-6-(2-chlorophenyl)-4-hydroxy-2,5-diazabicyclo[5.4.0]undeca-5,8,10,12-tetraen-3-one (IUPAC name); C<sub>15</sub>H<sub>10</sub>N<sub>2</sub>Cl<sub>2</sub>O<sub>2</sub> (molecular formula); 321.2 MW; CAS no. 846-9-1].**

$A_{\max}$ ) in relation to the accumulated UV energy ( $Q_{UV}$ ), calculated for each experimental set-up. All data used for the determination of peak area values are given in Table S1. The normalization attained with the  $Q_{UV}$  parameter allowed the comparison of the different LBPs increase/decrease profiles between the three experimental systems. Overall, it is also worth noting that since in most cases the different isomers could not be distinguished, their respective peak areas were presented as a global value. Exception noted for LBP291, for

which isomeric structures (a) and (b) were displayed separately.

As preliminary conclusions, two main aspects must be highlighted: (i) the SPP-CPCs photocatalytic system seemed to be the most efficient one amongst the three tested, since a faster LBP decrease was observed and the increase/decrease variations of several LBPs appeared at an earlier stage (Fig. 2). The slightly different initial LBP concentrations used – 2 ppm for SPP-CPCs vs. 6 and 5 ppm for LsTQUV photolysis and

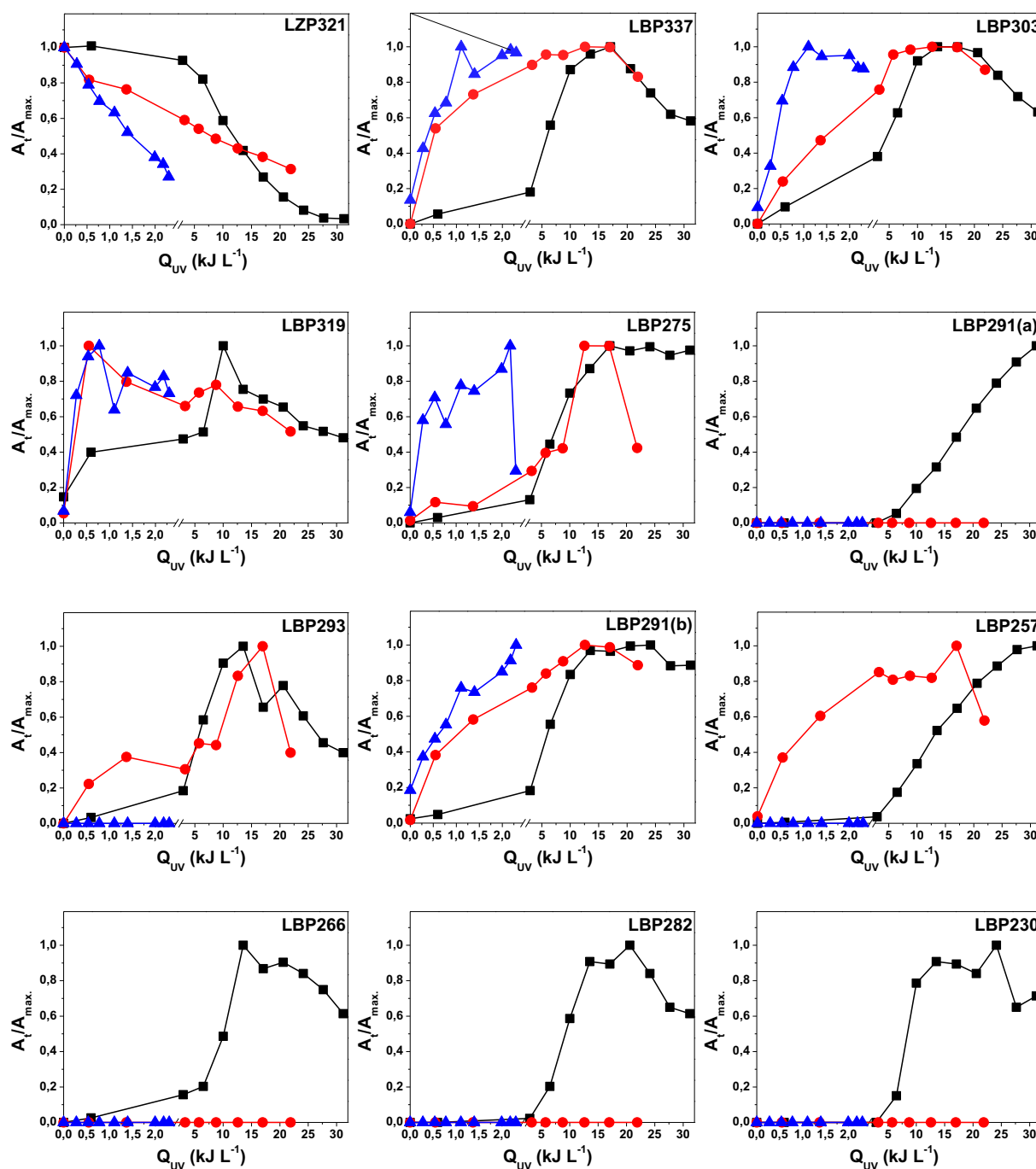


Fig. 2 – Graphical representation of LBP and respective LBPs evolution profiles, over the photo-treatment process in distilled water, in terms of ratio  $A_t/A_{\max}$ . (peak area at time  $t$ /maximal peak area) as a function of the amount of accumulated UV energy per liter of sample: ■ – Lab-scale TQ150W-UV prototype (LsTQUV); ● – Lab-scale Blacklight Blue-UV system (LsBLBUV); ▲ – Solar Pilot Plant with CPCs (SPP-CPCs).

LsBLBUV photocatalysis, respectively – are not expected to induce significant variations in either LZP photodegradation kinetics or LBPs evolution profiles. Moreover, SPP-CPCs highest efficiency, comparatively to the other experimental phototreatment systems, had already been demonstrated in previous works (Sousa et al., 2013); (ii) using this experimental system, some compounds such as LBP291(a), LBP257, LBP266, LBP282 and LBP230 were never detected. It remains to be clarified if this was due to the fact that the initial LZP concentration used in these experiments was lower than in the other two systems, or if the efficient degradation of LZP didn't allow isolating some intermediates.

Even departing from higher LZP initial concentrations in the case of UV lamp systems (in order to allow a proper LZP photodegradation kinetic follow-up, due to the highest lamp emission power compared to solar radiation), SPP-CPCs highest efficiency could be attributed to the improved radiation use, owing to CPCs geometrical dimensions/proportions, as well as to the outstanding differences between artificial and natural UV radiation spectra.

Lastly, the obtained evolution profiles for LBP337, LBP303, LBP319 and LBP275, regarding all three experimental set-ups, showed a noticeable increase as soon as light exposure began, which further reinforces the aforeproposed LZP photodegradation pathway. Moreover, their respective peak areas (data not shown) corresponded to the highest initial absolute values among all proposed LBPs' structures. Though we are perfectly aware that such comparison is not flawless, since different compounds will most likely present different MS responses, it is likely that the signal intensities should fall in a rather similar range, given that the basic structure is still maintained.

### 3.4. LZP photodegradation in a real WWTP effluent

The experimentally confirmed most effective LZP photodegradation system – 200 mg L<sup>-1</sup> TiO<sub>2</sub>-assisted photocatalysis using the SPP-CPCs system – was finally used to envisage LZP photofate in a real effluent sample. A preliminary physicochemical characterization (including some emerging pollutants) of this sample was performed and the results

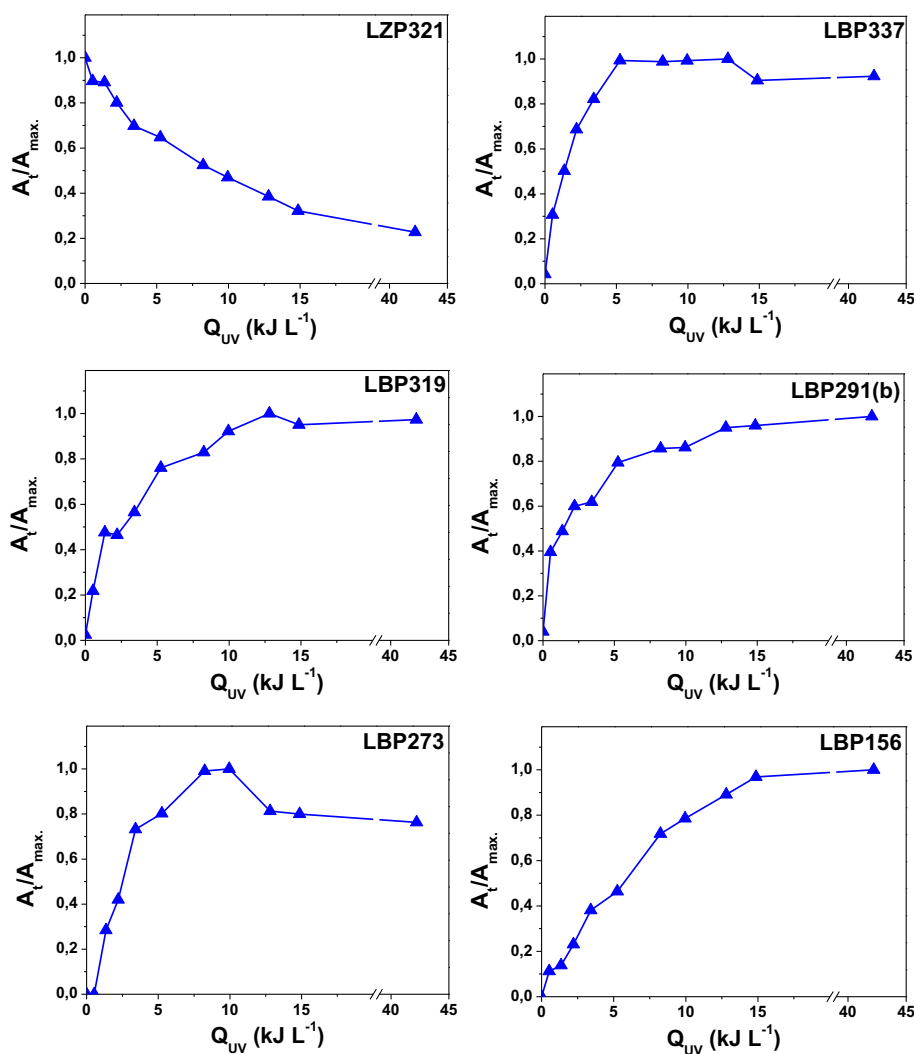


Fig. 3 – Graphical representation of LZP and respective LBPs evolution profiles, over the photo-treatment of a WWTP effluent using the SPP-CPCs set-up, in terms of ratio  $A_t/A_{max}$ . (peak area at time  $t$ /maximal peak area) as a function of the amount of accumulated UV energy per liter of effluent.



are displayed in Table S2. The effluent was further spiked with 2 mg L<sup>-1</sup> LZP, in order to facilitate the identification of potential LZP photoproducts. pH and temperature were constantly measured over the experiment, never falling outside the range of 6.35–7.10 and 18.5–28.5 °C (normal within-day variation), respectively.

The evolution profiles of the most abundant LBPs were then monitored and the charts obtained are presented in Fig. 3. It is well-known that nitrates, humic and fulvic acids present in wastewaters can act as sensitizers, giving rise to highly reactive species such as hydroxyl-radicals, singlet oxygen or H<sub>2</sub>O<sub>2</sub> and thus promoting indirect photolysis (Floesser-Mueller and Schwack, 2001). On the other hand, humic acids can also exert an optical filter effect, thereby attenuating the direct photolysis process. These two competing mechanisms are widely recognized and the overall effect is considered to be dependent on the analyte being investigated (Gonçalves et al., 2011; Lam and Mabury, 2005). However, even taking these aspects into consideration, no quantitative comparison with the results obtained for distilled water (Fig. 2) was possible. This holds true mainly due to the fact that the dissolved organic matter, present in the effluent sample, can render the analytes prone to different matrix effects. Nevertheless, from an overall analysis of Fig. 3, it can be observed that the photoproducts generated seem to be more persistent than LZP itself, requiring higher Q<sub>UV</sub> amounts to achieve their photodegradation. Consequently, some ecotoxicity tests would be quite relevant to further assess their environmental impact.

#### 4. Conclusions

The work presented herein allowed, for the first time, the elucidation of the photodegradation mechanism of LZP, a rather recalcitrant drug, often detected and quantified in the aquatic compartment. After LZP photo(catalytic) treatment using two lab-scale photochemical reactors and a Solar Pilot Plant with CPCs, the identification of its main photoproducts was carried out by ultra-high performance liquid chromatography coupled to high resolution mass spectrometry. Based on the concept of “diagnostic fragment ions” and accurate masses, six major LBPs were identified and elucidated, with nominal [M + H]<sup>+</sup> masses of 337, 303, 319, 275, 291 and 293 Da. The proposed photodegradation mechanism included the initial opening of LZP diazepinone seven-membered ring, followed by a rearrangement into a highly stabilized six-membered aromatic ring and subsequent cleavage and/or hydroxylation reactions.

Provided that the CPCs Solar Pilot Plant showed to be the most efficient system amongst the three tested, it was further applied to the treatment of a municipal WWTP effluent, where the generated LBPs proved to be more persistent than LZP itself. Accordingly, future experiments should comprise some bioassays, in order to evaluate the potential biological toxicity of the treated effluent.

#### Acknowledgments

The authors express their gratitude to IAREN – Water Institute of the Northern Region, LSRE – Laboratory of Separation and

Reaction Engineering and ICT – Institute of Chemical Technology, for technical and financial support. This work was partially supported by project PEst-C/EQB/LA0020/2011, financed by FEDER through COMPETE – *Programa Operacional Factores de Competitividade*, project PTDC/AAC-AMB/113091/2009, financed by FCT – *Fundação para a Ciência e a Tecnologia*, by funds of QREN – ON.2, O Novo Norte, through the research project NORTE-07-0162-FEDER-000022, and by specific university research MSMT No 21/2012. M.A. Sousa acknowledges her Doctoral fellowship (SFRH/BD/44509/2008) supported by FCT and co-financed by FSE/POPH (European Union).

#### Appendix A. Supplementary data

Supplementary data related to this article can be found at <http://dx.doi.org/10.1016/j.watres.2013.06.029>.

#### REFERENCES

- Budavari, S., O'Neil, M.J., Smith, A., Heckelman, P.E., 1989. *The Merck Index*, eleventh ed. Merck & CO., Inc., Rahway, N.J., U.S.A.
- Calisto, V., Domingues, M.R.M., Esteves, V.I., 2011. Photodegradation of psychiatric pharmaceuticals in aquatic environments – kinetics and photodegradation products. *Water Research* 45 (18), 6097–6106.
- Castiglioni, S., Bagnati, R., Calamari, D., Fanelli, R., Zuccato, E., 2005. A multiresidue analytical method using solid-phase extraction and high-pressure liquid chromatography tandem mass spectrometry to measure pharmaceuticals of different therapeutic classes in urban wastewaters. *Journal of Chromatography A* 1092 (2), 206–215.
- Coetsier, C.M., Spinelli, S., Lin, L., Roig, B., Touraud, E., 2009. Discharge of pharmaceutical products (PPs) through a conventional biological sewage treatment plant: MECs vs PECs? *Environment International* 35 (5), 787–792.
- Cooper, W.J., Mezyk, S.P., Peller, J.R., Cole, S.K., Song, W., Mincher, B.J., Peake, B.M., 2008. Studies in radiation chemistry: application to ozonation and other advanced oxidation processes. *Ozone: Science and Engineering* 30 (1), 58–64.
- Ferrer, I., Thurman, E.M., 2007. Multi-residue method for the analysis of 101 pesticides and their degradates in food and water samples by liquid chromatography/time-of-flight mass spectrometry. *Journal of Chromatography A* 1175 (1), 24–37.
- Floesser-Mueller, H., Schwack, W., 2001. Photochemistry of organophosphorus insecticides. *Reviews of Environmental Contamination and Toxicology* 172, 129–228.
- Galvez, J., Malato, S., 2003. *Solar Detoxification*; United Nations Educational, Scientific and Cultural Organization. UNESCO (electronic copy only).
- Gonçalves, C., Pérez, S., Osorio, V., Petrovic, M., Alpendurada, M.F., Barceló, D., 2011. Photofate of Oseltamivir (Tamiflu) and Oseltamivir Carboxylate under natural and simulated solar irradiation: kinetics, identification of the Transformation products, and environmental occurrence. *Environmental Science and Technology* 45 (10), 4307–4314.
- Gros, M., Petrovic, M., Barceló, D., 2006. Development of a multi-residue analytical methodology based on liquid-chromatography-tandem mass spectrometry (LC-MS/MS) for screening and trace level determination of pharmaceuticals in surface and wastewaters. *Talanta* 70 (4), 678–690.

- Gros, M., Petrovic, M., Ginebreda, A., Barceló, D., 2010. Removal of pharmaceuticals during wastewater treatment and environmental risk assessment using hazard indexes. *Environment International* 36 (1), 15–26.
- International Narcotics Control Board, U.N., 2010. Psychotropic Substances – Report 2009: Statistics for 2008, N.Y., U.S.A.
- Kasprzyk-Hordern, B., Dinsdale, R.M., Guwy, A.J., 2009. The removal of pharmaceuticals, personal care products, endocrine disruptors and illicit drugs during wastewater treatment and its impact on the quality of receiving waters. *Water Research* 43 (2), 363–380.
- Lacina, O., Urbanová, J., Poustka, J., Hajšlová, J., 2010. Identification/quantification of multiple pesticide residues in food plants by ultra-high-performance liquid chromatography-time-of-flight mass spectrometry. *Journal of Chromatography A* 1217 (5), 648–659.
- Lam, M.W., Mabury, S.A., 2005. Photodegradation of the pharmaceuticals atorvastatin, carbamazepine, levofloxacin, and sulfamethoxazole in natural waters. *Aquatic Sciences* 67 (2), 177–188.
- Lau, T.K., Chu, W., Graham, N.J.D., 2007. The aqueous degradation of butylated hydroxyanisole by  $UV/S_2O_8^{2-}$ : study of reaction mechanisms via dimerization and mineralization. *Environmental Science and Technology* 41 (2), 613–619.
- Malato, S., Fernández-Ibáñez, P., Maldonado, M.I., Blanco, J., Gernjak, W., 2009. Decontamination and disinfection of water by solar photocatalysis: recent overview and trends. *Catalysis Today* 147 (1), 1–59.
- Pereira, J.H.O., Vilar, V.J.P., Borges, M.T., González, O., Esplugas, S., Boaventura, R.A.R., 2011. Photocatalytic degradation of oxytetracycline using  $TiO_2$  under natural and simulated solar radiation. *Solar Energy* 85 (11), 2732–2740.
- Pinho, L.X., Azevedo, J., Vasconcelos, V.M., Vilar, V.J.P., Boaventura, R.A.R., 2012. Decomposition of *Microcystis aeruginosa* and Microcystin-LR by  $TiO_2$  oxidation using artificial UV light or natural sunlight. *Journal of Advanced Oxidation Technologies* 15 (1), 98–106.
- Richardson, S.D., Ternes, T.A., 2011. Water analysis: emerging contaminants and current issues. *Analytical Chemistry* 83 (12), 4614–4648.
- Rizzo, L., 2011. Bioassays as a tool for evaluating advanced oxidation processes in water and wastewater treatment. *Water Research* 45 (15), 4311–4340.
- Santos, J.L., Aparicio, I., Callejón, M., Alonso, E., 2009. Occurrence of pharmaceutically active compounds during 1-year period in wastewaters from four wastewater treatment plants in Seville (Spain). *Journal of Hazardous Materials* 164 (2–3), 1509–1516.
- Silva, B.F., Jelic, A., López-Serna, R., Mozeto, A.A., Petrovic, M., Barceló, D., 2011. Occurrence and distribution of pharmaceuticals in surface water, suspended solids and sediments of the Ebro river basin, Spain. *Chemosphere* 85 (8), 1331–1339.
- Sousa, M.A., Gonçalves, C., Pereira, J.H.O.S., Vilar, V.J.P., Boaventura, R.A.R., Alpendurada, M.F., 2013. Photolytic and  $TiO_2$ -assisted photocatalytic oxidation of the anxiolytic drug lorazepam (Lorenin® pills) under artificial UV light and natural sunlight: a comparative and comprehensive study. *Solar Energy* 87 (1), 219–228.
- Ternes, T.A., 1998. Occurrence of drugs in German sewage treatment plants and rivers. *Water Research* 32 (11), 3245–3260.
- Valcárcel, Y., Martínez, F., González-Alonso, S., Segura, Y., Catalá, M., Molina, R., Montero-Rubio, J.C., Mastroianni, N., López de Alda, M., Postigo, C., Barceló, D., 2012. Drugs of abuse in surface and tap waters of the Tagus River basin: heterogeneous photo-Fenton process is effective in their degradation. *Environment International* 41 (0), 35–43.
- Vilar, V.J.P., Capelo, S.M.S., Silva, T.F.C.V., Boaventura, R.A.R., 2011. Solar photo-Fenton as a pre-oxidation step for biological treatment of landfill leachate in a pilot plant with CPCs. *Catalysis Today* 161 (1), 228–234.
- Webb, S., Ternes, T., Gibert, M., Olejniczak, K., 2003. Indirect human exposure to pharmaceuticals via drinking water. *Toxicology Letters* 142 (3), 157–167.
- Zuehlke, S., Duennbier, U., Heberer, T., 2007. Investigation of the behavior and metabolism of pharmaceutical residues during purification of contaminated ground water used for drinking water supply. *Chemosphere* 69 (11), 1673–1680.